Proton branching ratios of ^{23}Mg levels

C. H. Kim (김찬희)[1], K. Y. Chae (채경육)[1,*] S. Ahn (안성훈)[2] D. W. Bardayan[3] K. A. Chipps[2,4,5] J. A. Cizewski[6] M. E. Howard[6] R. L. Kozub[7] M. S. Kwag (곽민식)[1] K. Kwak (곽규진)[8] B. Manning[6] M. Matos[9] P. D. O'Malley[6,3] S. D. Pain[5] W. A. Peters[10] S. T. Pittman[5] A. Ratkiewicz[6] M. S. Smith[5] and S. Strauss[6,3]

[1]*Department of Physics, Sungkyunkwan University, Suwon 16419, Republic of Korea*
[2]*Department of Physics and Astronomy, University of Tennessee, Knoxville, Tennessee 37996, USA*
[3]*Department of Physics, University of Notre Dame, Notre Dame, Indiana 46556, USA*
[4]*Department of Physics, Colorado School of Mines, Golden, Colorado 80401, USA*
[5]*Physics Division, Oak Ridge National Laboratory, Oak Ridge, Tennessee 37831, USA*
[6]*Department of Physics and Astronomy, Rutgers University, New Brunswick, New Jersey 08903, USA*
[7]*Department of Physics, Tennessee Technological University, Cookeville, Tennessee 38505, USA*
[8]*Department of Physics, School of Natural Science, Ulsan National Institute of Science and Technology (UNIST), Ulsan 44919, Republic of Korea*
[9]*Department of Physics and Astronomy, Louisiana State University, Baton Rouge, Louisiana 70803, USA*
[10]*Oak Ridge Associated Universities, Oak Ridge, Tennessee 37831, USA*

(Received 2 November 2021; accepted 27 January 2022; published 7 February 2022)

Background: The anomalous ^{22}Ne abundance measured in certain presolar graphite grains is thought to arise from the decay of ^{22}Na that was synthesized at high temperatures in core-collapse supernovas. To better interpret this abundance anomaly, the primary destruction mechanism of ^{22}Na, the ^{22}Na$(p,\gamma)^{23}$Mg reaction, must be better understood.
Purpose: Determine proton branching ratios of several ^{23}Mg excited states that play a role in the high-temperature ^{22}Na$(p,\gamma)^{23}$Mg reaction rate.
Methods: Particle decays of ^{23}Mg excited states populated with the previously reported ^{24}Mg$(p,d)^{23}$Mg transfer reaction measurement [Kwag *et al.*, Eur. Phys. J. A **56**, 108 (2020)] were analyzed to extract proton branching ratios. The reaction was studied using a 31-MeV proton beam from the Holifield Radioactive Ion Beam Facility of Oak Ridge National Laboratory and ^{24}Mg solid targets.
Results: Proton branching ratios of several ^{23}Mg excited states in the energy range $E_x = 8.044$-9.642 MeV were experimentally determined for the first time for the $p0$ and $p1'$ $(p1 + p2 + p3)$ decay channels.
Conclusions: These new branching ratios for ^{23}Mg levels can provide an experimental foundation for an improved high-temperature rate of the ^{22}Na$(p,\gamma)^{23}$Mg reaction needed to understand production of anomalously high ^{22}Ne abundance in core-collapse supernovas.

DOI: 10.1103/PhysRevC.105.025801

I. INTRODUCTION

The radionuclide ^{22}Na ($t_{1/2} = 2.6$ y) can be synthesized during nova and supernova explosions. In novas, ^{22}Na is created via either the ^{21}Ne$(p,\gamma)^{22}$Na reaction or the β^+ decay of ^{22}Mg [1,2]. When ^{22}Na β-decays to the first excited state of ^{22}Ne, the characteristic 1.275-MeV γ ray follows. This γ ray is a target of several current and future space-based γ-ray telescopes including the International Gamma-Ray Astrophysics Laboratory (INTEGRAL) [3], Advanced Compton Telescope (ACT) [4], and enhanced ASTROGAM [5]. In core-collapse supernovas, ^{22}Na is mainly created through the ^{21}Ne$(p,\gamma)^{22}$Na reaction [6]. A high abundance ratio of ^{22}Ne in presolar graphite grains is thought to mainly originate from core-collapse supernovas. This is the so-called Ne-E(L) anomaly as the abundance is notably different from the solar abundance [6–9]. The ^{22}Na$(p,\gamma)^{23}$Mg reaction is believed to play a crucial role in understanding the destruction of ^{22}Na during both nova and supernova explosions. As the reaction proceeds through resonances in ^{23}Mg, the spectroscopic information of resonant states located above the proton threshold at 7.581 MeV is required to estimate the ^{22}Na$(p,\gamma)^{23}$Mg reaction rate. Owing to this importance, many studies have been conducted on the energy levels of ^{23}Mg [10–18].

One of the important properties needed to estimate the reaction rate is the proton branching ratio. In recent studies that utilized β-delayed proton emissions of ^{23}Al, for instance, the proton decay branching ratios of a few ^{23}Mg levels were obtained at energies near $E_x = 7.8$ MeV [14,15,17,18] which provide critical information for the ^{22}Na$(p,\gamma)^{23}$Mg reaction rate calculations. As the proton threshold energy of ^{23}Mg is 7.581 MeV [19], the energy levels studied in those

*kchae@skku.edu; FAX: +82-31-290-7055.

references fall in the Gamow window for $T = 0.1$-0.5 GK, which corresponds to nova temperatures. In Ref. [17], β-delayed proton emission spectra at higher energy regions were obtained. However, as the transition intensities were normalized to that of the 451-keV line, more studies on the proton branching ratios of populated ^{23}Mg levels are required to estimate the $^{22}\mathrm{Na}(p,\gamma)^{23}\mathrm{Mg}$ reaction rate accurately at high temperatures.

In the present work, the proton decay branching ratios of several ^{23}Mg levels populated from a previously reported $^{24}\mathrm{Mg}(p,d)^{23}\mathrm{Mg}$ transfer reaction study [20] were investigated as a follow-up analysis. The reaction was measured to help determine the astrophysical $^{22}\mathrm{Na}(p,\gamma)^{23}\mathrm{Mg}$ reaction rate at nova temperatures. The angular distributions of deuterons from the reaction were extracted to constrain the spins and parities of the populated ^{23}Mg energy levels. The spin value of $J^{\pi} = 5/2^{+}$ for the 7.788-MeV level, which is the dominant resonance for the $^{22}\mathrm{Na}(p,\gamma)^{23}\mathrm{Mg}$ reaction at nova temperatures, was adopted in the reaction rate calculations. The result showed that the updated reaction rate was approximately a factor of 3 smaller than that from the literature at $T = 0.3$ GK. Because many ^{23}Mg energy levels in the range $E_x = 6.537$-9.642 MeV were observed in Ref. [20] through the (p,d) transfer reaction, the current analysis of the proton branching ratios can significantly enhance our knowledge of the high-temperature burning of the radionuclide ^{22}Na.

II. EXPERIMENT

The experimental setup was described in detail in Ref. [20]. A 31-MeV proton beam at an intensity of ≈ 60 pA was produced at the Holifield Radioactive Ion Beam Facility at Oak Ridge National Laboratory. The beam bombarded an isotopically enriched (>99.9%) ^{24}Mg solid target with an areal density of ≈ 520 μg/cm^2. A large-area silicon detector array (SIDAR) [21] was placed at forward angles to detect charged particles from the $^{24}\mathrm{Mg}(p,d)^{23}\mathrm{Mg}$ transfer reactions. A thick (9.5-mm) aluminum plate with a 19-mm-diam hole was placed directly in front of the target ladder to protect the fragile silicon detectors from the halo of the intense beam. The SIDAR comprised four trapezoidal wedges of $\Delta E - E$ telescopes. Each telescope was configured with a 100-μm-thick energy loss (ΔE) detector backed by a 1000-μm residual energy (E) detector for standard energy loss techniques. The angles covered by the detector array were $16.8^{\circ} \leqslant \theta_{\mathrm{lab}} \leqslant 44.8^{\circ}$. The energy response of each silicon strip was calibrated using an α-emitting source composed of ^{239}Pu (5.157 MeV), ^{241}Am (5.486 MeV), and ^{244}Cm (5.805 MeV). The energy resolutions were measured to be approximately 1% for the α particles. Deuterons from the $^{24}\mathrm{Mg}(p,d)^{23}\mathrm{Mg}$ reaction were clearly identified using the standard energy loss techniques. To better reconstruct the excitation energies, internal energy calibrations were also performed using six well-known ^{23}Mg energy levels: the ground state and excited states at $E_x =$ 2.359, 2.771, 5.286, 5.992, and 9.642 MeV. A total of 17 ^{23}Mg levels were identified at excitation energies less than approximately 9.7 MeV.

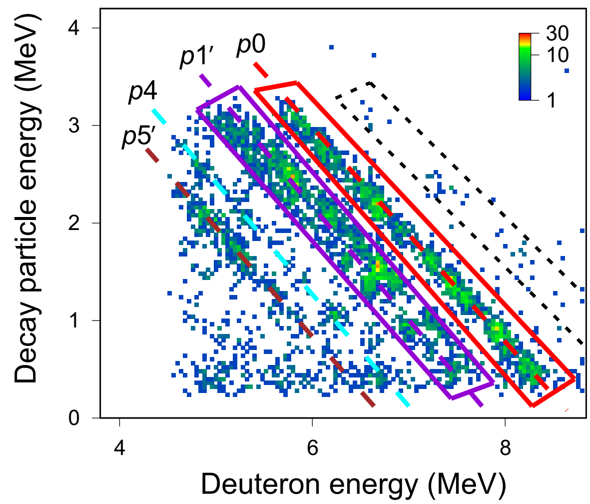

FIG. 1. Decay particle energy versus coincident reaction deuteron energy plot for all identified events. Four major diagonal bands labeled as $p0$, $p1'$, $p4$, and $p5'$ are evident. Each band represents a proton decay channel. Only the events falling in the red and purple gates were used to determine branching ratios, and are associated with the ground state ($p0$) and three closely located levels of ^{22}Na at $E_x = 582.8$, 657.0, and 890.9 keV ($p1'$), respectively. The weak band in the black dotted gate shows the decay events originated from the impurity of the target.

III. RESULTS AND ANALYSIS

A. Coincident events

Events from the proton decay of ^{23}Mg were identified by requiring coincidence between the deuterons from the $^{24}\mathrm{Mg}(p,d)^{23}\mathrm{Mg}$ reaction and the decay protons. When two charged particles fell within an event window of ≈ 4 μs, the events were considered coincident. Decay protons stopped at the first layer of the detectors (ΔE) were analyzed in the present work. A decay proton energy versus coincident reaction deuteron energy plot for all identified events is shown in Fig. 1. By considering the coincidence, only ^{23}Mg nuclei produced from the $^{24}\mathrm{Mg}(p,d)^{23}\mathrm{Mg}$ reaction could be considered in the present analysis. Proton decays of ^{23}Mg that originate from other possible reaction mechanisms such as the $^{24}\mathrm{Mg}(p,2n)^{23}\mathrm{Al}$ reaction followed by β decays of ^{23}Al were excluded by detecting the deuterons instead of the ^{23}Mg recoils.

As shown in Fig. 1, four major diagonal bands are evident. Each diagonal band represents a proton decay channel: the $p0$ channel for the decay to the ground state of ^{22}Na; $p1'$ for a combined channel of three closely spaced final levels of ^{22}Na at $E_x = 582.8$, 657.0, and 890.9 keV ($p1$, $p2$, and $p3$); $p4$ for the decay to the ^{22}Na level at 1527.7 keV; and $p5'$, again, for a combined channel of three closely spaced final levels at 1937.0, 1951.7, and 1983.1 keV ($p5$, $p6$, and $p7$). The closely spaced energy levels in the $p1'$ and $p5'$ groups could not be fully resolved in the present analysis. The events located to the left of the $p5'$ channel are thought to be decay protons from higher proton decay channels overlapped with α decay channels, exhibiting no clear bands. Background events consist of

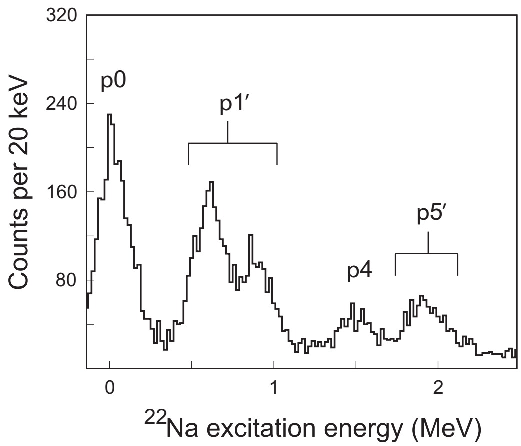

FIG. 2. Reconstructed ^{22}Na excitation energy spectrum from the proton-deuteron coincidences in Fig. 1. The peaklike structures labeled as $p1'$ and $p5'$ are associated with three closely spaced levels each that could not be fully resolved in the present work.

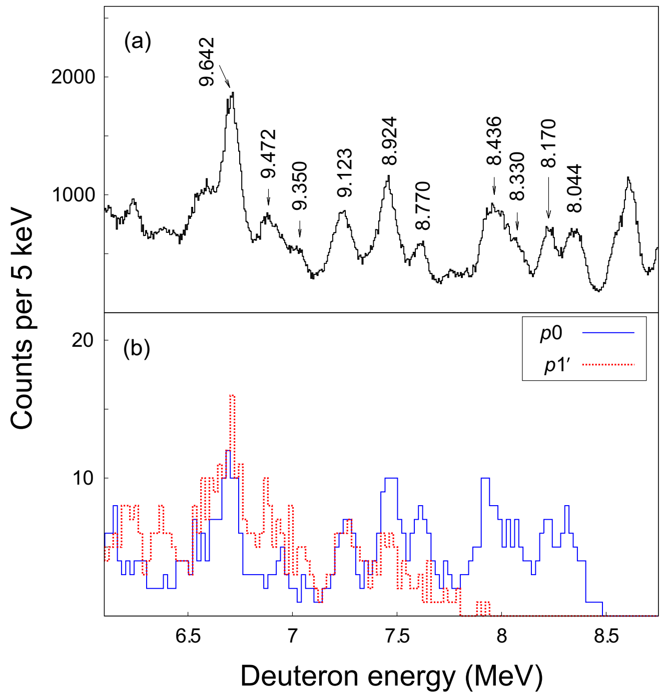

FIG. 3. (a) Deuteron energy spectrum obtained from the ^{24}Mg(p,d)^{23}Mg reaction measurement [20]. Identified ^{23}Mg levels are labeled with their excitation energies in MeV. (b) Gated spectra of the coincident protons for the $p0$ (blue solid line) and $p1'$ (red dotted line) channels.

decay protons from the impurities in the target and random coincidences. For instance, a possible proton decay channel of ^{15}O, which was populated by ^{16}O(p,d)^{15}O, to the ground state of ^{14}N can be found in Fig. 1 (black dotted box). It did not affect the current analysis as the band is not overlapped with the ^{23}Mg proton decay channels. The decay protons from the other potential impurities such as ^{12}C are energetically far away from the energy region of interest. Because some random coincidences were evident at deuteron energies higher than those relevant for the events in the rightmost gate of Fig. 1, where particle decay is energetically forbidden, another gate was implemented in this region to estimate the level of random coincidences. The ^{22}Na excitation energy was reconstructed using the energies of the coincident particles for each identified event. The results are shown in Fig. 2.

B. Decay-gated spectra and branching ratios

Figure 3(a) shows the deuteron single spectrum obtained from the previous ^{24}Mg(p,d)^{23}Mg measurement [20]. The excitation energies reported in the reference are indicated in MeV for several identified levels in this deuteron energy range. Figure 3(b) shows the spectra gated on the $p0$ and $p1'$ groups in Fig. 1.

For the first step of the branching ratio estimation, each identified peak in Fig. 3(a) was Gaussian fitted. Then, the corresponding peak in the decay-gated spectra was also fitted to obtain the number of proton decay events using the same parameters such as the centroid and width. The geometric detection efficiency ($\approx 2\%$) obtained by assuming isotropic decay was also used in the branching ratio estimations. A discussion of the isotropy assumption is presented in Sec. III C. By comparing the number of decay-gated events to that of deuteron singles for each identified ^{23}Mg level in the energy range $E_x = 8.044$-9.642 MeV, the proton branching ratios of

TABLE I. Proton branching ratios (b_p) of ^{23}Mg levels extracted for $p0$, $p1'$, $p1$, $p2$, and $p3$. The excitation energy values were taken from Ref. [20]. Uncertainties include factors originated from the statistics, backgrounds, and discrepancy between isotropic and anisotropic decay. See Sec. III C for detailed argument on isotropic and anisotropic decay.

E_x (keV)	b_{p0}	$b_{p1'}$	b_{p1}	b_{p2}	b_{p3}
8044 ± 4	0.36 ± 0.11				
8170 ± 4	0.36 ± 0.12				
8330 ± 6	0.48 ± 0.15				
8436 ± 7	0.59 ± 0.18				
8770 ± 8	0.86 ± 0.27				
8924 ± 5	0.47 ± 0.15	0.26 ± 0.08	(0.13 ± 0.04)	(0.01 ± 0.01)	(0.12 ± 0.04)
9123 ± 7	0.36 ± 0.11	0.35 ± 0.11	(0.06 ± 0.02)	(0.27 ± 0.09)	(0.03 ± 0.01)
9642	0.37 ± 0.11	0.49 ± 0.15	(0.14 ± 0.05)	(0.26 ± 0.08)	(0.08 ± 0.03)

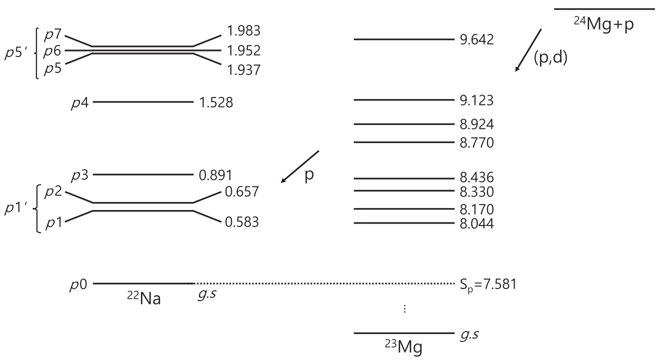

FIG. 4. A diagram of the involved energy levels of ^{22}Na and ^{23}Mg along with decay channels. Energies are in units of MeV.

several transitions in the $p0$ and $p1'$ channels could be obtained. The corresponding results are summarized in Table I. The uncertainty due to the isotropic assumption had the largest contribution to the total uncertainty of each branching ratio (see Sec. III C). The statistical uncertainty was less than 10% of the total uncertainty in most cases. The random background contribution was approximately 4% for b_{p0} of $E_x = 8.044$ and 8.170 MeV and $b_{p1'}$ of $E_x = 8.924$ MeV, whereas those for the other branching ratios were negligible. The diagram of the relevant energy levels and decay channels is shown in Fig. 4.

Several peaks apparent in the deuteron singles were not included in the proton branching ratio estimations because of poor statistics. Although the energy levels at $E_x = 9.350$ and 9.472 MeV were clearly identified in Ref. [20], for instance, the corresponding peaks in the decay-gated proton energy spectrum were rather featureless and therefore could not be well fitted. The branching ratios for the $p4$ and $p5'$ channels were not extracted, as the excitation energies of the ^{23}Mg levels associated with those channels are higher than those reported in the previous study [20], except for the states at $E_x = 9.123$ and 9.642 MeV. Although these states are located above the thresholds of $p4$ and $p5'$ channels, the decay energies were too small to observe or no legitimate peak was obtained.

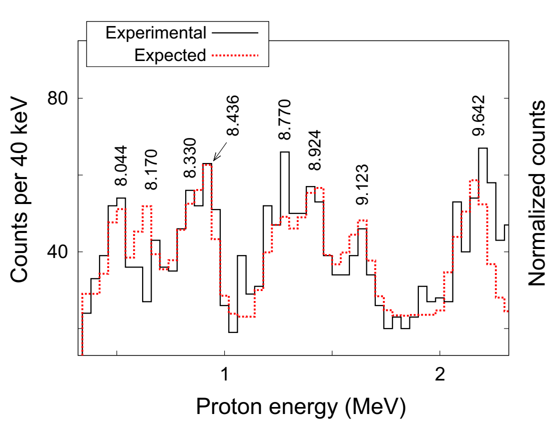

FIG. 5. Proton energy spectrum for the coincident events falling in the $p0$ gate (black solid line). Identified ^{23}Mg energy levels are labeled with their excitation energies in MeV. The expected proton energy spectrum (displayed as the red dotted line) well reproduces the experimental result.

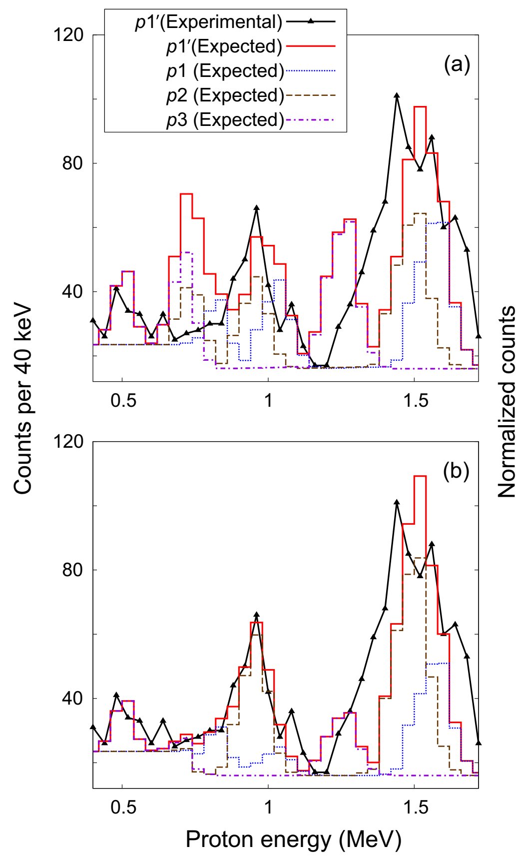

FIG. 6. Similar to Fig. 5, the empirical proton energy spectrum for the $p1'$ channel (black solid line). (a) The expected proton energy spectra obtained by assuming equal contributions from three final levels are also shown. (b) The expected spectra after the fit are shown (see text).

The proton energy spectrum of the coincident events obtained for the $p0$ channel is shown in Fig. 5 as a black solid line. The excitation energies of ^{23}Mg associated with several identified peaks are indicated in MeV. The expected proton energy spectrum is also displayed as the red dotted line in the figure. This spectrum was obtained in the following manner. Relativistic kinematics calculations were performed by considering the excitation energies in ^{23}Mg, angular distributions of deuterons, and proton branching ratios extracted in the present work. The production of deuterons through the ^{24}Mg$(p,d)^{23}$Mg transfer reaction and isotropic proton decay of ^{23}Mg levels were assumed in the calculations. As shown in the figure, the empirical proton energy spectrum can be well reproduced for the $p0$ channel, indicating that the extracted branching ratio values are well estimated.

Because the $p1'$ channel contains three final states in ^{22}Na that were not fully resolved in the present work, the expected proton energy spectrum for the channel could not be reconstructed using the same method as that for the $p0$ channel analysis. As the first approach, the proton energy spectrum was calculated by assuming equal contributions from three levels to the obtained $p1'$ branching ratios summarized in

TABLE II. Observed and calculated proton energies and their uncertainties for identified transitions. All proton energies are in keV.

	$p0$ (keV)		$p1'$ (keV)			
	Expected	Measured	Expected			Measured
E_x (keV)	E_f = g.s.		E_f = 583 keV ($p1$)	657 keV ($p2$)	891 keV ($p3$)	
8044	498 ± 60	510 ± 95				
8170	653 ± 72	709 ± 65				
8330	800 ± 29	841 ± 15				
8436	899 ± 110	940 ± 59				
8770	1289 ± 129	1285 ± 98				
8924	1441 ± 36	1448 ± 49	843 ± 33	751 ± 40	525 ± 39	589 ± 142
9123	1631 ± 130	1642 ± 96	1051 ± 43	975 ± 42	726 ± 39	1003 ± 120
9642	2180 ± 235	2231 ± 15	1588 ± 62	1513 ± 60	1275 ± 56	1554 ± 155

Table I. The calculated spectrum is shown in Fig. 6(a) with the experimental result. The calculated proton energies, along with the corresponding observed energies, are summarized in Table II for the 11 identified transitions. Three apparent peaks in the experimental spectrum that are located at $E_p =$ 0.589, 1.003, and 1.554 MeV are associated with the transitions from ^{23}Mg levels at $E_x = 8.924$, 9.123, and 9.642 MeV, respectively.

As shown in Fig. 6(a), some of the expected peaks notably differ from the empirical results at the corresponding proton energy regions. To fit the expected result to the empirical one, the branching ratios of the $p1$, $p2$, and $p3$ channels ($E_f = 0.583$, 0.657, and 0.891 MeV) were parametrized. The best fitting result is shown in Fig. 6(b). The contributions from the $p1$, $p2$, and $p3$ channels to the $p1'$ branching ratio were determined through the fitting. The results are presented in Table I as individual branching ratios. The uncertainty contribution from statistics was less than 50% in these branching ratios. Results show that the transitions from the $E_x = 8.924$ MeV state through the $p2$ channel and the one from the $E_x = 9.123$ MeV state through the $p3$ channel are rather weak to have the branching ratios of less than 5%. Strong branches were obtained for the transitions associated with the $p2$ channel except for the one from the $E_x = 8.924$ MeV state.

C. Isotropic and anisotropic decay

The relative angle (i.e., the angle between the reaction deuteron and decay proton) was deduced for each identified decay event for the $E_x = 8.924$ (9.642) MeV level through the $p0$ ($p1'$) decay as shown in the top (bottom) panel of Fig. 7. Because the angular distributions of decay protons could not be sufficiently obtained owing to limited statistics, an isotropic decay in the center of mass frame was assumed for the branching ratio calculations. Moreover, because the laboratory and the center of mass frames are similar in the case of normal kinematics, isotropic decay in the laboratory frame could be used instead. As the decay protons are emitted at each angle with the same probability under this assumption, the expected intensity as a function of the relative angle can be derived from the angular distribution of deuterons.

The calculated distributions for $E_x = 8.924$ and 9.642 MeV levels are shown as black solid lines in the top and

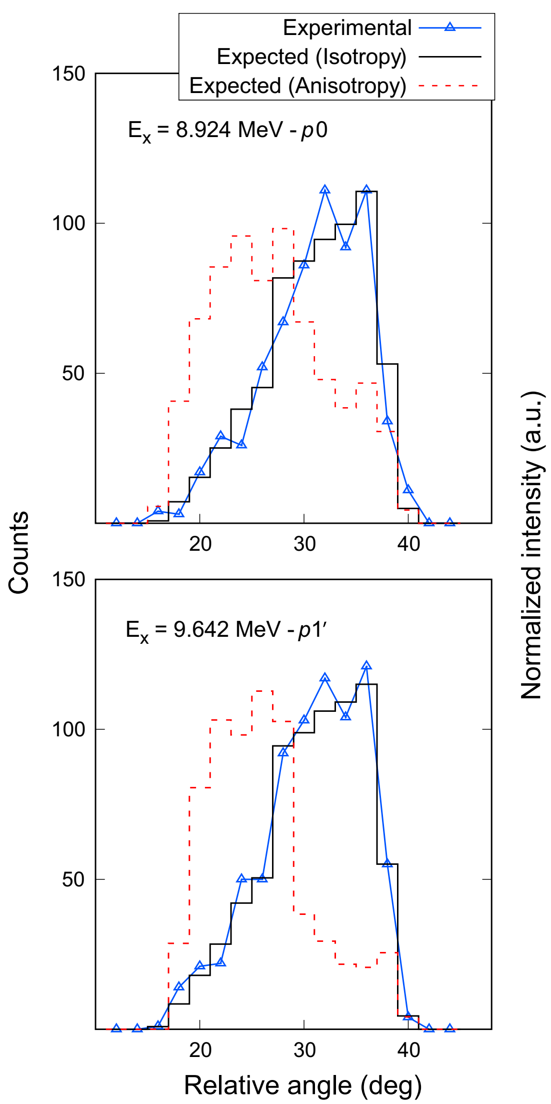

FIG. 7. Counts of decay protons from the 8.924-MeV (9.642-MeV) level as a function of relative angle for the $p0$ ($p1'$) channel shown in the top (bottom) panel as a blue solid line. The expected distributions assuming isotropic and anisotropic decay of protons are shown as a black solid and a red dotted line, respectively.

bottom panels of Fig. 7, respectively. While the transitions from unbound levels in ^{23}Mg would be mostly anisotropic except for $l = 0$ transfer, the assumption of isotropy resulted in good agreement between the empirical and calculated distributions. As previously done in Refs. [22,23], a relative angle histogram for anisotropic decay was also considered by assuming a sinusoidal variation, as indicated by the red dashed line in the figure. The results show that assuming the isotropic decays for the observed transitions is reasonable. Nevertheless, the conservative systematic uncertainty of 30% was introduced for the extracted branching ratios to account for any possible discrepancies between isotropic and anisotropic decays, as has been done in Refs. [22,23].

IV. ASTROPHYSICAL ^{22}Na$(p,\gamma)^{23}$Mg REACTION RATE

For novas, states in ^{23}Mg just above the proton binding energy are dominant resonances for the proton capture reaction ^{22}Na$(p,\gamma)^{23}$Mg. Even with the results from direct measurements of the reaction, the reaction rate still remains uncertain [10,11,13]. Several previous studies implemented indirect measurements using β-delayed decay of ^{23}Al have been performed as well, focusing on the state near $E_x \approx$ 7.8 MeV [14,15,17,18]. They measured the proton branching ratio as it is critically concerned with the partial widths of the state ($b_p = \Gamma_p/\Gamma_{\mathrm{tot}}$) and, correspondingly, the resonance strength. Most recently, Friedman *et al.* [18] reported the proton branching ratio value of $6.5(8) \times 10^{-3}$ for the $E_x = 7.79$ MeV level, which is a factor of 5 lower compared to the previous value. This shows the importance of precise estimations on the proton branching ratios of ^{23}Mg.

For core-collapse supernovas, investigations on the properties of higher lying states are required as they have much higher temperatures compared to novas. For the most part, only the upper limits of the resonance strengths could be deduced through the direct measurements [10,11]. An indirect study using ^{22}Na $+p$ resonant scatterings estimated two resonance strengths of $E_x = 8.793(13)$ and 8.916(15) MeV by relying on the shell-model calculations [24]. They calculated the strengths by assuming $\Gamma_{p0}/\Gamma_{\mathrm{tot}} \approx 1$. If the two states are the same states with the ones at $E_x = 8.770(8)$ and 8.924(5) MeV in the current measurements, the resonance strengths will be lowered by factors of 0.86 and 0.47, respectively, which would lower the ^{22}Na$(p,\gamma)^{23}$Mg reaction rate from their estimate [24]. The current branching ratios can be useful to calculate the strengths of additional resonances. However, the other critical nuclear properties of the states needed to calculate the partial widths, including spin parities and half-lives, are mostly unknown. Additional measurements or theoretical model calculations are therefore needed to determine a new proton capture rate on ^{22}Na at supernova temperatures.

V. CONCLUSION

As a follow-up analysis of previously reported ^{24}Mg$(p,d)^{23}$Mg reaction measurements, decay protons from excited states in ^{23}Mg were investigated to obtain proton branching ratios of the populated levels. By detecting the reaction products and decay particles simultaneously, several proton decay branches of ^{23}Mg levels could be identified: the $p0$ channel for the decay to the ground state of ^{22}Na and the $p1'$ channel for the three closely spaced levels at $E_x = 582.8$, 657.0, and 890.9 keV.

Proton branching ratios for eight (three) transitions associated with the $p0$ ($p1'$) channel were obtained for the energy levels in ^{23}Mg in the range $E_x = 8.044$-9.642 MeV. Isotropic decay in the center of mass frame was assumed and the geometric detection efficiency was considered in the branching ratio calculations. Proton decay of ^{23}Mg levels to higher lying states in ^{22}Na was also observed. However, the corresponding branching ratios could not be extracted because the peaks of interest were not obtained. Excitation energies of the levels investigated in the present work correspond to $E_{\mathrm{c.m.}} \approx$ 0.4-2 MeV for the astrophysical ^{22}Na$(p,\gamma)^{23}$Mg reaction rate, which is relevant for core-collapse supernova scenarios. The impact of these branching ratios on the high-temperature ^{22}Na$(p,\gamma)^{23}$Mg thermonuclear reaction rate will be explored in the future with additional measurements.

ACKNOWLEDGMENTS

This work was supported by the National Research Foundation of Korea (NRF) grants funded by the Korea government (MSIT) (Grants No. 2013M7A1A1075764, No. 2016R1A5A1013277, and No. 2020R1A2C1005981). Additionally, the research was supported in part by the National Nuclear Security Administration under the Stewardship Science Academic Alliances program through the U.S. DOE Cooperative Agreement No. DE-FG52-08NA28552 with Rutgers University and Oak Ridge Associated Universities. This work was also supported in part by the Office of Nuclear Physics, Office of Science of the U.S. DOE under Contract No. DE-FG02-96ER40955 with Tennessee Technological University, Contract No. DE-FG02-96ER40983 with the University of Tennessee, and Contract No. DE-AC05-00OR22725 with Oak Ridge National Laboratory; by the National Science Foundation under Contract No. PHY-2011890 with University of Notre Dame and Contract No. PHY-1812316 with Rutgers University; and by the Institute for Basic Science (Grant No. IBS-R031-D1).

[1] J. José, A. Coc, and M. Hernanz, Astrophys. J. **520**, 347 (1999).
[2] A. L. Sallaska, C. Wrede, A. García, D. W. Storm, T. A. D. Brown, C. Ruiz, K. A. Snover, D. F. Ottewell, L. Buchmann, C. Vockenhuber, D. A. Hutcheon, J. A. Caggiano, and J. José, Phys. Rev. C **83**, 034611 (2011).
[3] M. Hernanz and J. José, New Astron. Rev. **48**, 35 (2004).
[4] S. E. Boggs, New Astron. Rev. **50**, 604 (2006).
[5] A. De Angelis *et al.*, J. High Energy Astrophys. **19**, 1 (2018).
[6] S. Amari, Astrophys. J. **690**, 1424 (2009).
[7] D. C. Black, Geochim. Cosmochim. Acta **36**, 347 (1972).

[8] S. Amari, A. Anders, A. Virag, and E. Zinner, Nature (London) **345**, 238 (1990).
[9] P. R. Heck, S. Amari, P. Hoppe, H. Baur, R. S. Lewis, and R. Wieler, Astrophys. J. **701**, 1415 (2009).
[10] S. Seuthe, C. Rolfs, U. Schröder, W. H. Schulte, E. Somorjai, H. P. Trautvetter, F. B. Waanders, R. W. Kavanagh, H. Ravn, M. Arnould, and G. Paulus, Nucl. Phys. A **514**, 471 (1990).
[11] F. Stegmüller, C. Rolfs, S. Schmidt, W. H. Schulte, H. P. Trautvetter, and R. W. Kavanagh, Nucl. Phys. A **601**, 168 (1996).
[12] H. Comisel, C. Hategan, G. Graw, and H. H. Wolter, Phys. Rev. C **75**, 045807 (2007).
[13] A. L. Sallaska, C. Wrede, A. García, D. W. Storm, T. A. D. Brown, C. Ruiz, K. A. Snover, D. F. Ottewell, L. Buchmann, C. Vockenhuber, D. A. Hutcheon, and J. A. Caggiano, Phys. Rev. Lett. **105**, 152501 (2010).
[14] R. J. Tighe, J. C. Batchelder, D. M. Moltz, T. J. Ognibene, M. W. Rowe, J. Cerny, and B. A. Brown, Phys. Rev. C **52**, R2298 (1995).
[15] K. Peräjärvi, T. Siiskonen, A. Honkanen, P. Dendooven, A. Jokinen, P. O. Lipas, M. Oinonen, H. Penttilä, and J. Äystö, Phys. Lett. B **492**, 1 (2000).
[16] V. E. Iacob, Y. Zhai, T. Al-Abdullah, C. Fu, J. C. Hardy, N. Nica, H. I. Park, G. Tabacaru, L. Trache, and R. E. Tribble, Phys. Rev. C **74**, 045810 (2006).
[17] A. Saastamoinen, L. Trache, A. Banu, M. A. Bentley, T. Davinson, J. C. Hardy, V. E. Iacob, M. McCleskey, B. T. Roeder, E. Simmons, G. Tabacaru, R. E. Tribble, P. J. Woods, and J. Äystö, Phys. Rev. C **83**, 045808 (2011).
[18] M. Friedman, T. Budner, D. Pérez-Loureiro, E. Pollacco, C. Wrede, J. José, B. A. Brown, M. Cortesi, C. Fry, B. Glassman, J. Heideman, M. Janasik, M. Roosa, J. Stomps, J. Surbrook, and P. Tiwari, Phys. Rev. C **101**, 052802(R) (2020).
[19] M. Wang, W. J. Huang, F. G. Kondev, G. Audi, and S. Naimi, Chin. Phys. C **45**, 030003 (2021).
[20] M. S. Kwag *et al.*, Eur. Phys. J. A **56**, 108 (2020).
[21] D. W. Bardayan, J. C. Blackmon, W. Bradfield-Smith, C. R. Brune, A. E. Champagne, T. Davinson, B. A. Johnson, R. L. Kozub, C. S. Lee, R. Lewis, P. D. Parker, A. C. Shotter, M. S. Smith, D. W. Visser, and P. J. Woods, Phys. Rev. C **63**, 065802 (2001).
[22] K. A. Chipps, S. D. Pain, U. Greife, R. L. Kozub, C. D. Nesaraja, M. S. Smith, D. W. Bardayan, A. Kontos, L. E. Linhardt, M. Matos, S. T. Pittman, and P. Thompson (JENSA Collaboration), Phys. Rev. C **95**, 044319 (2017).
[23] M. J. Kim, K. Y. Chae, S. Ahn, D. W. Bardayan, S. M. Cha, K. A. Chipps, J. A. Cizewski, M. E. Howard, R. L. Kozub, K. Kwak, B. Manning, M. Matos, P. D. OMalley, S. D. Pain, W. A. Peters, S. T. Pittman, A. Ratkiewicz, M. S. Smith, and S. Strauss, Phys. Rev. C **104**, 014323 (2021).
[24] S. J. Jin, Y. B. Wang, J. Su, S. Q. Yan, Y. J. Li, B. Guo, Z. H. Li, S. Zeng, G. Lian, X. X. Bai, W. P. Liu, H. Yamaguchi, S. Kubono, J. Hu, D. Kahl, H. S. Jung, J. Y. Moon, C. S. Lee, T. Teranishi, H. W. Wang, H. Ishiyama, N. Iwasa, T. Komatsubara, and B. A. Brown, Phys. Rev. C **88**, 035801 (2013).